Materials Science & Engineering C 107 (2020) 110273

Contents lists available at ScienceDirect

Materials Science & Engineering C

journal homepage: www.elsevier.com/locate/msec

Cu-nanoflower decorated gold nanoparticles-graphene oxide nanofiber as electrochemical biosensor for glucose detection

Seung Hoon Baek[a,1], Jihyeok Roh[a,1], Chan Yeong Park[a], Min Woo Kim[a], Rongjia Shi[a], Suresh Kumar Kailasa[b], Tae Jung Park[a,*]

[a] Department of Chemistry, Institute of Interdisciplinary Convergence Research, Research Institute of Chem-Bio Diagnostic Technology, Chung-Ang University, 84 Heukseok-ro, Dongjak-gu, Seoul, 06974, Republic of Korea
[b] Department of Applied Chemistry, Sardar Vallabhbhai National Institute of Technology, Surat, 395007, Gujarat, India

ARTICLE INFO

Keywords:
Cu-nanoflower@AuNPs-GO nanofibers
Glucose monitoring
Nano-bio hybrid
Electrochemical sensor

ABSTRACT

A novel electrospinning approach is proposed for the fabrication of copper (Cu)-nanoflower decorated gold nanoparticles (AuNPs)-graphene oxide (GO) nanofiber (NF) as an electrochemical biosensor for the glucose detection. In this study, GO was mixed with poly(vinyl alcohol) (PVA) and used as a fiber precursor, which greatly improves the electrochemical properties. The above solution was uniformly coated onto the surfaces of gold chip to form GO NFs *via* electrospinning. AuNPs were coated onto the surface of GO NFs and then incorporated organic-inorganic hybrid nanoflower [Cu nanoflower-glucose oxidase (GOx) and horseradish peroxidase (HRP)]. The electrochemical experiments revealed that Cu-nanoflower@AuNPs-GO NFs exhibited outstanding electrochemical catalytic nature, and selectivity for the conversion of glucose to gluconic acid in the presence of GOx-HRP-Cu nanoflower. The Cu-nanoflower@AuNPs-GO NFs coated Au chip exhibited good linear range 0.001–0.1 mM, with a detection limit of 0.018 μM. The Cu-nanoflower@AuNPs-GO NFs modified Au chip exhibited higher catalytic properties, which are attributed to the coating of unique organic-inorganic nanostructured materials on the surfaces of Au chip. These results indicate that the nano-bio hybrid materials can be applied as a promising electrochemical biosensor to monitor glucose levels in biofluids.

1. Introduction

Glucose plays an essential role in numerous metabolic pathways of humans that produces adenosine triphosphate. However, abnormal (higher) levels of glucose in biofluids cause several serious complications such as blindness, heart disease, high blood pressure and kidney failure [1,2]. Thus, monitoring of glucose levels in biofluids has shown significant importance in biomedical research to prevent and control diabetes. The interest of the monitoring of glucose levels in biofluids using glucose oxidase enzyme has attracted much attention due to several advantages such as selectivity, simplicity and rapidity. In view of this, glucose oxidase has been used in the development of various analytical approaches including quantum dots-based fluorescence [3], electrochemical [4], optical [5], chemiluminescence sensor [6] and surface plasmon resonance [7] for the glucose detection in biological samples. Among these techniques, electrochemical sensor have shown remarkable merits such as higher sensitivity, rapidity, cost-effcitiveness and selectivity for the detection of glucose in various sample matrices [8,9]. It also proves that portable electrochemical device has been fabricated for bioassays, which could be operated by unskillful person at minimal volume of samples [10]. Importantly, electrochemical biosensor based on glucose enzyme reactions has played a major role in the continuous monitoring of glucose levels in personal glucometers [11].

Enzymatic electrochemical sensors have found to be promissing tools for the analysis of clinically important molecules due to their high sensitivity, good selectivity [12,13], water-solubility and low toxicity [14]. To enhance electrocatalytic activity and selectivity, many studies have been used enzymes-coated electrochemical sensors for the detection of wide variety of molecules from complex samples [15]. At the same time, the free enzymes have some limitations at certain conditions such as pH, temperature, which yields electrochemical sensor with poor reproducibility, low operational stability and unstable responsibility [16,17]. However, these limitations are successfully overcome by immobilizing enzymes on the solid supports, offering several advantages such as high enzyme-to-substrate ratio, great enzyme stability, reusability and good diagnosis, which also facilitates to reduce diagnosis

* Corresponding author.
E-mail address: tjpark@cau.ac.kr (T.J. Park).
[1] These authors equally contributed to this work.

https://doi.org/10.1016/j.msec.2019.110273
Received 14 August 2019; Received in revised form 21 September 2019; Accepted 2 October 2019
Available online 14 October 2019
0928-4931/

time with remarkably. Recently, immobilization of enzyme on various nanostructured materials (nanoparticles [18], organic or inorganic composites [19,20] and 3-dimensional materials [21]) has received significant attention in electrochemical sensors due to improve selectivity and enzyme activity towards selected target analytes. Moreover, protein-inorganic hybrid nanoflowers have shown to be efficient electrochemical sensors for sensitive analysis of various molecules [22]. The immobilization of enzymes on the nanoflowers also exhibit remarkably advantages such as improvement of enzyme activity, stability, durability and reusability with spacious large surface-to-volume ratio of the nanoflowers [23]. Importantly, enzyme-immobilized nanomaterials-based electrochemical sensors exhibited better analytical features than that of pure enzyme-based electrochemical sensors [24,25]. Therefore, the integration of novel organic-inorganic nanostructured materials with electrodes may open up a simplest way to establish biosensors with significant analytical features.

Electrospinning is a simple and emerging technology for the fabrication of fibrous nanostructured materials in the range of nanometers to micrometers from wide variety of polymers [26]. It is a simple process to decorate inorganic nanomaterials, which yields to change the morphology and surface area for unique bioapplications [27]. Recent years, nanofibers (NFs) have been attracted as promissing materials to integrate with various analytical techniques such as fluorescence [28], electrochemical device [29], UV-visible spectrometry [30] and drug delivery/tracing [31] for qualitative and quantitative analysis of various target analytes due to long storage stability, flexibility and large surface area. Among many polymers, poly(vinyl alcohol) (PVA) is a water soluble polymer and widely used in various industrial applications because of its nontoxicity, low cost, eco-friendliness, chemical resistance and biological compatibility due to pendant hydroxyl groups. To fabricate NFs using PVA, various crosslinking methods including irradiation [32], heating [33], chemical treatments [34] have been used for the preparation of water insoluble NFs. Because of its low electrical conductivity, it might be difficult to use in the development of electrochemical sensors. Recently, PVA was combined with chitosan and GO, studied their biocompatibility towards ATDC5 cells [35]. After going through the literature survey, no reports were attempted to fabricate AuNPs-decorated glucose oxidase NFs (GO NFs) with copper nanoflowers for the development of electrochemical biosensor. In this study, a facile and sensitive electrochemical biosensor was developed for the detection of glucose by modifying the gold chip with Cu-nanoflower-AuNPs-decorated GO NFs. First, GO NFs were synthesized on the gold chip by electrospinning method (Scheme 1). Then, GO NFs were further decorated with AuNPs *via* electrostatic interaction, which enhances the conductivity of GO NFs and sensitivity for glucose detection. Since metal NPs with NFs improves thermal resistance, mechanical strength and electrical properties, which can also offer to use as biosensor. Finally, GOx-HRP-Cu-nanoflower were deposited on AuNPs-GO NFs (Cu-nanoflower@AuNPs-GO NFs) and then above NFs were coated on the gold chip using 1% Nafion as a binding agent (Scheme 1). When glucose is added into the system, it reacts with O_2 in the presence of Cu-nanoflower@AuNPs-GO NFs, resulting to generate H_2O_2 *via* enzymatic catalytic reaction, which is remarkably increased electric current (Fig. S1). As a result, Cu-nanoflower@AuNPs-GO NFs showed remarkable electrochemical responses to the glucose concentration, allowing to develop glucose sensor with high selectivity and sensitivity. Thus, Cu-nanoflower@AuNPs-GO NFs could open a simple electroanalytical platform for glucose detection in biofluids.

2. Materials and methods

2.1. Chemicals

Polyvinyl alcohol [(-CH_3CHOH-)$_n$, MW 22,000], D(+)-glucose (98%) and sucrose ($C_{12}H_{22}O_{11}$) were purchased from Junsei (Tokyo, Japan). Copper (II) sulfate pentahydrate ($CuSO_4{\cdot}5H_2O$, 99.9%), calcium chloride ($CaCl_2$, anhydrous, 96.0%), L(+)-ascorbic acid, D(+)-sucrose (Saccharose), urea, and hydrogen peroxide (H_2O_2) were obtained from Samchun (Seoul, Korea). Potassium chloride (KCl) and sodium chloride (NaCl) were obtained from Duksan (Ansan, Korea). Peroxidase from horseradish, gold (III) chloride trihydrate ($HAuCl_4{\cdot}3H_2O$), permanganate ($KMnO_4$), potassium persulfate ($K_2S_2O_8$), phosphorus pentoxide (P_2O_5), concentrated sulfuric acid (Conc. H_2SO_4), cysteamine hydrochloride and glucose oxidase from *Aspergillus niger* were purchased from Sigma-Aldrich (St. Louis, MO, USA) and used without any further purification. Sodium borohydride ($NaBH_4$) was purchased from Daejung Chemicals (Siheung, Korea). Bovine serum albumin (BSA) was purchased from GenDEPOT (Katy, TX, USA). Fetal bovine serum (FBS) obtained from Gibco (Waltham, MA, USA). Graphite powder was purchased from Kanto Chemical (Kanto, Japan).

2.2. Preparation of AuNPs-GO NFs

PVA (25 g) was dissolved into DI water (100 mL) by continuous stirring at 80 °C for 6 h to make 25 wt% PVA solution. GO (1 mg) was added to DI water (1 mL) and sonicated for 30 min to make homogenous GO solution. Then, 1.0 mg/mL of GO solution was added into 25 wt% of PVA solution at 1:10 (v/v) ratio and stirred for 3 h at room

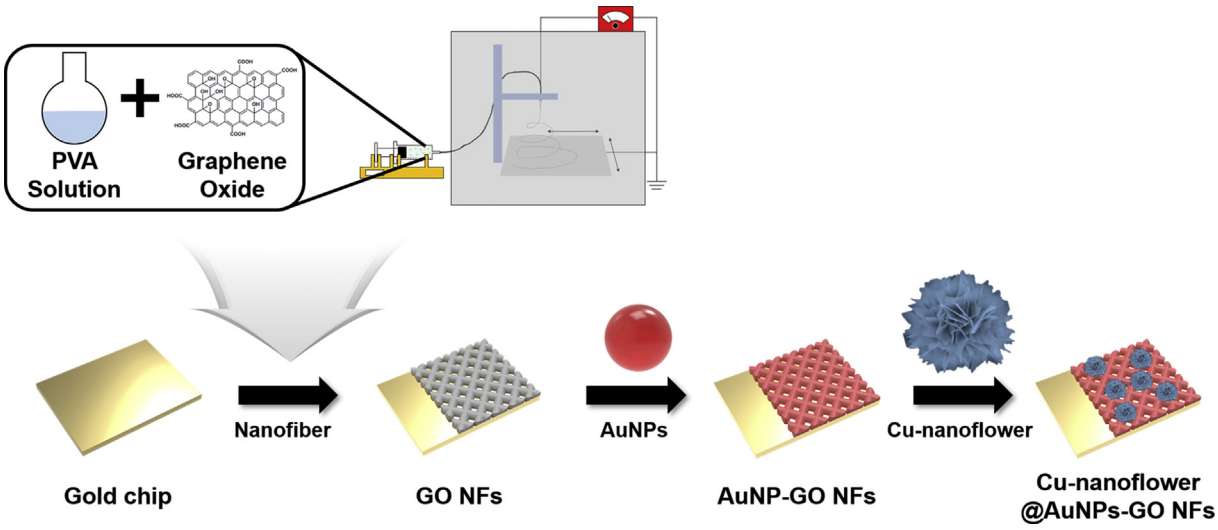

Scheme 1. Schematic illustration for the fabrication of Cu-nanoflower@AuNPs-GO NFs-based electrochemical glucose nano-biosensor.

temperature. To deposit on Au chip, PVA/GO solution was sprayed with 22-G needle by electrospinning using syringe pump flowrate at 1.0 mL/h under high voltage (15 kV). Electrospun GO NFs coated Au chips directly collected after 10 min electrospinning, and the needle tip-to-collector distance was 15 cm. After electrospinning process, GO NFs were calcined in a dry oven at 180 °C for 1 h to make NFs insoluble. And then, 200 μL of cysteamine-AuNPs solution (9 nM) was dropped onto the surfaces of GO NFs and kept stand at room temperature for 1 h. The resulting AuNPs-GO NFs were washed with DI water three times to remove the unbound AuNPs, and dried at 60 °C.

2.3. Cu-nanoflower decorated AuNPs-GO NFs (Cu-nanoflower@AuNPs-GO NFs)

Cu-nanoflowers were synthesized as per the following procedure. Briefly, 1.0 mg/mL of GOx and 0.05 mg/mL of horseradish peroxidase (HRP) were added into phosphate-buffered saline (PBS). To this, 120 mM of $CuSO_4$ solution (20 μL) was added and then stirred at room temperature for 3h. After that, the solution was incubated at room temperature for 72 h and then washed with PBS for 5 times. The synthesized Cu-nanoflowers were stored at 4 °C for further use. To fabricate Cu-nanoflower@AuNPs-GO NFs as an electrochemical biosensor, 40 μg/mL of nanoflower solution (10 μL) was dropped on AuNPs-GO NFs and dried at room temperature. To bind Cu-nanoflower@AuNPs-GO NFs onto the surface of Au chip, 1% of Nafion in 2-propanol (3 μL) was used as a binding agent to bind Au chip with Cu-nanoflower@AuNPs-GO NFs that used as working electrode for the glucose sensing.

2.4. Cu-nanoflower@AuNPs-GO NFs-based electrochemical detection of glucose

The Cu-nanoflower@AuNPs-GO NFs-based electrochemical biosensor was established by the following procedure. A small amount (typically 50 μL) of glucose solution (0.001–0.1 mM) was injected into a 5 mL of electrochemical cell that contains Cu-nanoflowers@AuNPs-GO NFs Au-chip electrode and 0.1 M of PBS (pH 5.0) as a working electrolyte and their electrochemical measurements were performed on a CHI 750E instrument (CH Instruments, Austin, TX, USA) using a conventional 3-electrode cell. The reference electrode was Ag/AgCl and the counter electrode was a platinum electrode. Chronoamperometry and CV current measurements were performed in 0.1 M of PBS solution (pH 5.0). The CV was recorded from −0.8 V to +0.6V at a sweep speed of 0.02 V/s. Chronoamperometry measurements were recorded under an applied potential of −0.25 V (vs. Ag/AgCl). Moreover, the continuous addition of glucose at different concentration was performed for redundancy measurement and construction of calibration, however total addition did not exceed 500 μL to avoid significant changes in electrolyte composition.

2.5. Characterization

UV-visible absorption spectra were measured on a JASCO 670 spectrophotometer (Tokyo, Japan). Field emission scanning electron microscope (FE-SEM) images were taken by using SIGMA instrument from Carl Zeiss (Cambridge, UK). Field emission transmittance electron microscope (FE-TEM) images were taken by using JEM-F200 from JEOL (Tokyo, Japan). Fourier transform infrared (FT-IR) spectra were recorded on a JASCO 6660FV (Tokyo, Japan). X-ray diffraction (XRD) patterns of the samples were measured on a D8-Advance instrument from Bruker AXS (Karlsruhe, Germany) with Cu Kα radiation at room temperature (40 kV and 40 mA). Raman spectra were performed by using Kaiser optical system form Raman Rxn 1 (Ann Arbor, MI, USA). Electrospinning process was performed by electrospinning system (NNC-ESDR; NanoNC, Seoul, Korea).

3. Results and discussion

3.1. Optimization and characterization of GO nanofiber

The as-synthesized GO NFs were characterized by using UV-visible, FT-IR and Raman spectroscopic techniques, respectively. Fig. S2a represents that UV-visible spectrum of GO shows two absorption peaks at 230 nm and the shoulder peak at 300 nm due to n-π* transition of C═O bonds and π-π* transition of C═C bonds [36]. The FT-IR spectrum of GO showed the characteristic peaks at 480, 1035, 1577, 1736, and 3400 cm^{-1}, which are attributed to the characteristic functional groups i.e., C-H, C-O, C═C, C═O and O-H in GO, respectively (Fig. S2b). These results confirmed that carbonyl, epoxide and hydroxyl groups are present in the GO [37]. In the other hand, graphite powder did not show any characteristic absorption peaks for the above groups. The Raman spectrum of GO shows the two special peaks at 1350 (D) and 1590 (G) cm^{-1} were attributed to the E_{2g} mode of sp^2 carbon atoms and the symmetry A_{1g} mode of GO (Fig. S2c). The peak at 2680 cm^{-1} belongs to two-dimensional (2D) sp^2 carbon hexagonal networks of GO [38]. Based on the above results, GO was successfully synthesized.

The development of GO NFs as a promising electrochemical biosensor is strongly dependent on the morphology and composition of GO-PVA mixture. Therefore, the effect of PVA and GO concentrations, voltage and syringe pump flowrate were investigated on the NFs morphology and diameter by studying field emission scanning microscopy (FE-SEM). Initially, we fixed the concentration of GO and PVA at 1 mg/mL 1:10 (v/v) ratio, 15 cm as tip-to-collector distance, applied voltage 15 kV and solution flowrate at 1.0 mL/h. To identify the optimal concentration of PVA, the different concentration of PVA (10–25 wt%) were added into GO solution and performed electrospinning. The formed GO NFs were analyzed by FE-SEM. It can be seen that the bead detects were noticed on GO NFs when PVA concentration was from 10 to 20 wt% (Figs. S3a–c). On the other hand, 25 wt% of PVA concentration was decreased bead defects and the formed GO NFs are homogenous with smooth surface and uniform diameter (Fig. S3d). Based on this, we fixed 25 wt% of PVA solution as optimum concentration. Fig. S4 represents that the FE-SEM image of GO NFs at different applied voltage from 10 to 17 kV. It can be seen that drop defect could not be observed in the formed GO NFs at higher voltage, which is due to the formation of strong coulombic force between tip and collector [39]. Fig. S4e shows that the measured diameter of GO NFs by FE-SEM. It was noticed that the diameter of GO NFs is gradually decreased with increasing voltage up to 17 kV. As voltage increased, error range of fiber diameter also decreased. At 15 kV, uniform size of NFs was obtained. Thus, 15 kV was selected as an optimum voltage for uniform diameter of GO NFs. Then, we also investigated that the effect of syringe pump flowrate for the formation of GO NFs (Fig. S5). Importantly, bead defects were appeared on NFs at higher flowrate 1.5 mL/h. Thus, 25 wt% PVA solution, applied voltage 15 kV and flowrate 1.0 mL/h were selected as a best condition for fabrication of GO NFs by electrospinning.

Furthermore, the effect of GO concentration (0.1–2.0 mg/mL) in GO NFs was investigated for sensitive electrochemical detection of glucose using FE-SEM and electrochemical impedance spectroscopy (EIS). FE-SEM images of GO NFs revealed that the no major changes were observed in the morphology of GO NFs with increasing concentration of GO (Fig. S6). Fig. 1a shows that the impedance values of GO NFs at different concentrations of GO. It can be seen that the impedance values are decreased with increasing GO concentration up to 1.0 mg/mL and then reached to plateau, revealing the GO has greatly improved the electric conductivity of PVA-based NFs. Thus, we selected 1.0 mg/mL of GO as an optimum concentration for preparation of GO NFs. As shown in Fig. 1b, FT-IR spectrum of PVA NFs did not show any peak, however GO NFs show the characteristic peaks for functional groups hydroxyl, carboxyl and epoxide, confirming the formation of GO NFs.

Electrospinning cross-linking step was needed to develop water

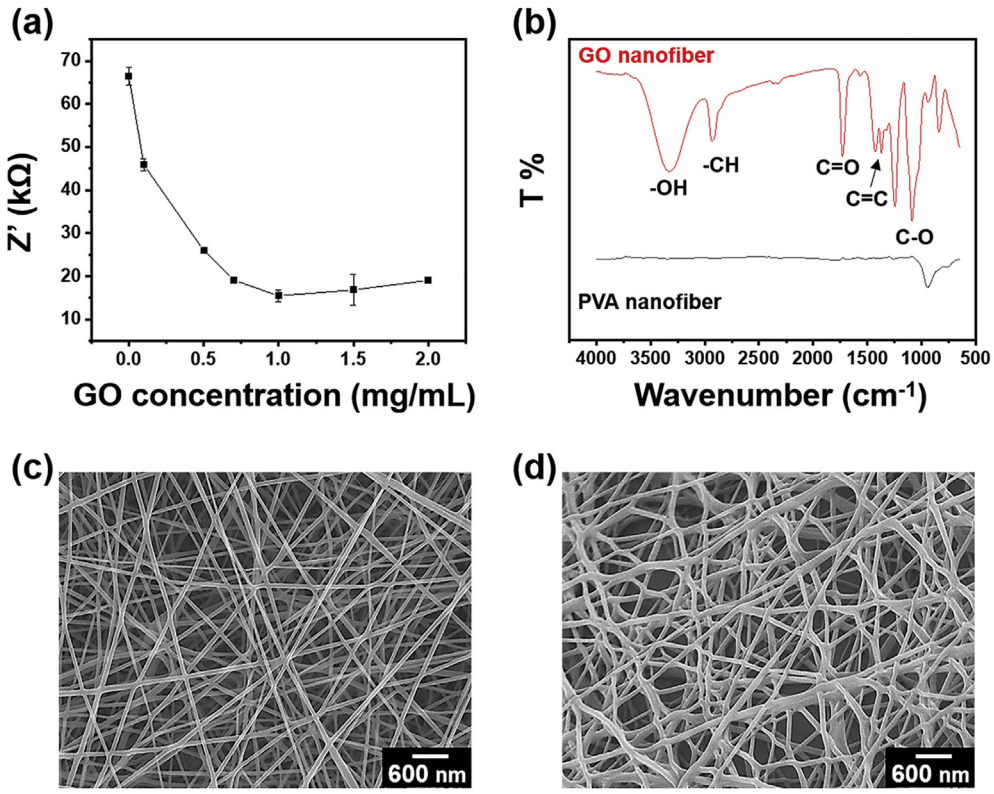

Fig. 1. Characterization of GO NFs. (a) Electrochemical impedance value of PVA NFs at different concentrations of GO (control – 2.0 mg/mL). (b) FT-IR spectra of GO NFs and PVA NFs. Characterization of calcined GO NFs. FE-SEM images of GO NFs (c) before and (d) after calcination.

stable GO NFs-based electrochemical sensor since PVA is a water-soluble polymer. To prepare GO NFs water stable, GO NFs were calcined at 180 °C for 1 h. After calcination, the crystallinity of PVA was increased due to the rearrangement of PVA chains. Furthermore, the calcined PVA has good mechanical properties at dry and wet state when compared to chemical crosslinked PVA [40]. As a result, water-insoluble GO NFs were obtained without change in the morphology (Fig. 1c and d). The calcined GO NFs are insoluble in water whereas non-calcined GO NFs are freely solution in water, which were confirmed by FE-SEM (Fig. S7). We also measured that the diameter of calcined- and un-calcined GO NFs by FE-SEM, revealing the diameter of calcined GO NFs (~168 nm) is slightly higher than that of un-calcined GO NFs (138 nm), which is in good agreement with other studies reported in the literature [41]. Therefore, water insoluble GO NFs were successfully synthesized for further applications.

3.2. Decoration of GO NFs with AuNPs

To increase sensitivity for glucose sensing, AuNPs were doped on the surface of GO NFs. GO NFs exhibits negative charge and the AuNPs show positive charge, resulting strong electrostatic force, which yields to decorate AuNPs on the surfaces of GO NFs. As shown in Fig. S8a, cysteamine-AuNPs showed absorption peak at 525 nm, which was ascribed to the surface plasmon resonance of AuNPs. As shown in Fig. S8b and Fig. S8c, the diameter of cysteamine-AuNPs was 20 nm, and zeta potential of cysteamine-AuNPs was positive 34.20 mV, respectively. Energy-dispersive X-ray spectroscopy (EDX) result shows the synthesized nanoparticle composed by Au (Fig. S8d).

The doping of AuNPs is carried out by dropping cysteamine-AuNPs solution on the GO NFs surface at different time intervals (10, 30, 60, 90, 120, 150 min). To find the best optimum time for doping of AuNPs on GO NFs, FE-SEM, UV-vis reflectance spectra, and XRD were studied. As shown in Fig. 2, cysteamine-AuNPs were well doped on the surface of GO NFs via electrostatic force. It was noticed that the characteristic crystalline peak of AuNPs was noticed in the XRD spectrum of AuNPs decorated GO NFs whereas that peak was absent in undoped GO NFs (Fig. S9a). Furthermore, AuNPs shows that characteristic peak at $\lambda = 500$ nm in the reflectance spectrum. According this, reflectance peak at 490 nm was gradually decreased with increasing doping time from 10 to 60 min and then reached to plateau (Fig. S9b). Similarly, impedance value of GO NFs was decreased by doping of AuNPs, reaching plateau at 60 min (Fig. S9c), suggesting the maximum amount of AuNPs were doped on the surface of GO NFs at 60 min.

3.3. Preparation of Cu-nanoflower@AuNPs-GO NFs

The formation mechanism for Cu-nanoflower follows the nucleation and growth process [42]. At the early stage, while Cu^{2+} ion forms copper phosphate crystal by interacting with phosphate anion in PBS solution, amide backbone in protein (GOx and HRP) coordinate with the crystal then formed the Cu-protein complex [24]. The complex act as seeds for the nanoflower, and these nuclei grow over the reaction time and form the petals of nanoflower. As following a series of these sequential reactions, a multi-layered structure of nanoflower could be composed. The growth of Cu-nanoflower was optimized by using different concentrations of Cu^{2+} ion (1.2, 12, 60, 120 and 180 mM) and GOx (0.3, 0.5, 0.7 and 1.0 mg/mL) *via* FE-SEM. As shown in Fig. S10, Cu-nanoflowers were not grown at lower concentration of Cu^{2+} ion (1.2 mM), however Cu-nanoflowers were formed with increasing concentration of Cu^{2+} ion from 12 to 180 mM, which can also notice that the formation of petals and flowers like morphology. The best morphology of Cu-nanoflowers was observed at 120 mM of Cu^{2+} ion and at higher concentration (180 mM) leads to degradation of Cu-nanoflowers. The effect of GOx concentration (0.3, 0.5, 0.7, 1.0 mg/mL) was also investigated on the formation of Cu-nanoflowers by FE-SEM (Fig. 3). Based on this result, 1.0 mg/mL of GOx was found to be the best concentration for the preparation of Cu-nanoflowers with uniform size. At the optimized condition at 1.0 mg/mL of GOx and 120 mM of Cu^{2+} ion,

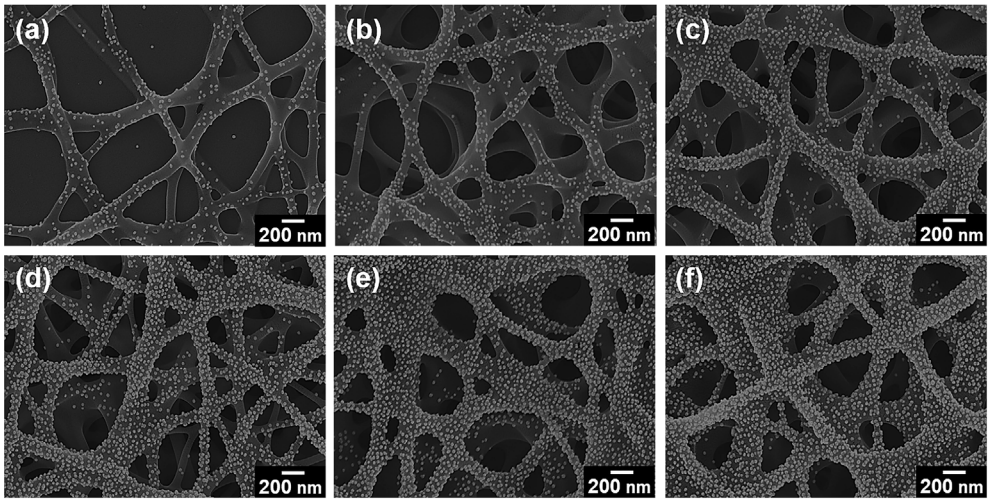

Fig. 2. FE-SEM images of AuNPs-GO NFs at different reaction times, (a) 10, (b) 30, (c) 60, (d) 90, (e) 120, and (f) 150 min.

FE-TEM images show a flower shape and uniform morphology as shown in Fig. S11.

3.4. Cu-nanoflower@AuNPs-GO NFs-based electrochemical detection of glucose

To verify whether the prepared Cu-nanoflower@AuNPs-GO NFs presents better performance then only Cu-nanoflowers, the electrodes which modified by each sample were analyzed by cyclic voltammetry technique in presence of 30 μM of glucose (Fig. 4a). The voltammogram of all samples shows that the pair of redox peaks (peak I/peak II) at −0.26/-0.028 V which related to the Au oxidation and reduction. However, another pair of peaks (peak I'/peak II") which may involve in the formation of incipient hydrous gold oxides $[Au^{+}(H_2O)_n]_{ads}$ pre-monolayer and the reduction of Au(I) hydrous oxide to Au adatoms [43] were occurred except the case of AuNPs-GO NFs due to the absence of glucose oxidase. Cu-nanoflower shows a small redox peak to response glucose, but AuNPs-GO NFs represents no significant response to glucose. With the synthesis of Cu-nanoflower@GO NFs, it was possible to further strengthen the signal of Cu-nanoflower because GO NFs combines gold chips with Cu-nanoflower. Moreover, AuNPs decorated Cu-nanoflower@GO NFs, which enhance the redox peak of Cu-nanoflower@GO NFs by its peroxidase-like activity. The Cu-nanoflower reacts with the glucose itself, combining with the GO NFs, and AuNPs make more synergetic effects. Based on the GO NFs as a supporter, its stability was strengthened. As the 3D-structured AuNPs lead to the expansion of its surface area, an intrinsic peroxidase-like activity could assist HRP to enhance the electrochemical activities. Among the samples representing that redox peak, Cu-nanoflower@AuNPs-GO NFs especially shows the highest cathodic current than others at the same amount of glucose.

Before assessing the electrochemical performance of Cu-nanoflower@AuNPs-GO NFs towards glucose, experimental conditions were established as follows. Firstly, the influence of the concentration

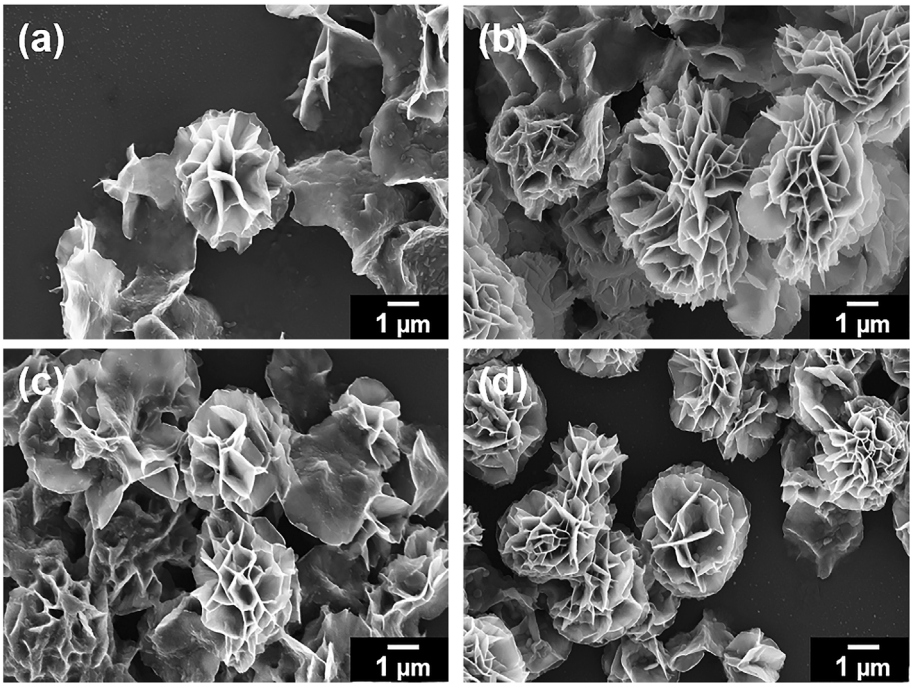

Fig. 3. Optimization of Cu-nanoflower at different GOx concentrations (a) 0.3, (b) 0.5, (c) 0.7, and (d) 1.0 mg/mL. Each nanoflowers were synthesized under same condition except GOx concentration (The concentrations of Cu^{2+} ion and HRP are 120 mM and 0.05 mg/mL).

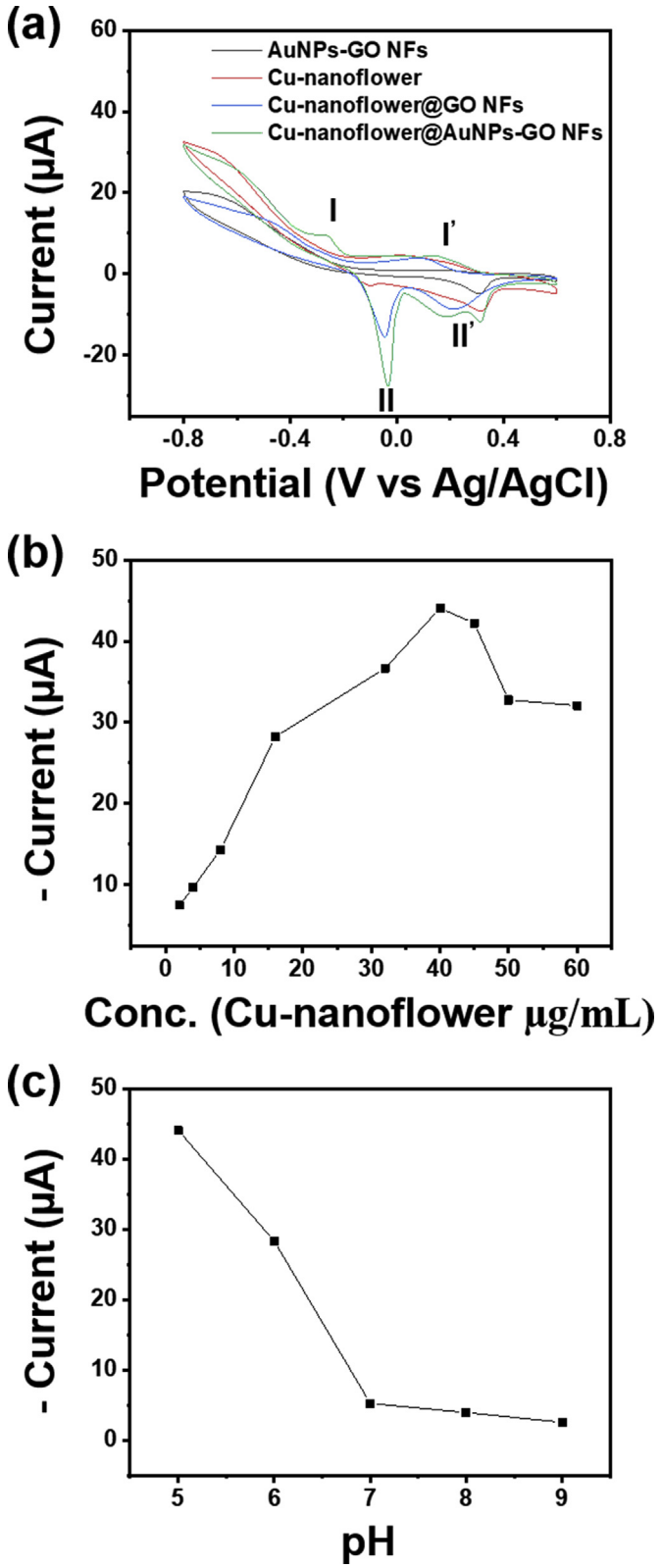

Fig. 4. (a) Cyclic voltammogram of working electrodes modified with GO NFs, Cu-nanoflowers, Cu-nanoflower@GO NFs and Cu-nanoflower@AuNPs-GO NFs in 30 μM of glucose at a scan rate of 20 mV/s. The optimization of Cu-nanoflower@AuNPs-GO NFs working electrode: The current measurement of the enzyme electrode in 50 μM glucose (b) with different concentrations of Cu-nanoflowers, (c) with varying pH environment.

of Cu-nanoflowers on AuNPs-GO NFs was investigated with a fixed amount of glucose (50 μM). As shown in Fig. 4b, while the current is gradually increased with a rising concentration of Cu-nanoflowers up to 40 μg/mL, and then decreased due to the insulation effect. Although Cu-nanoflowers are the key material for the recognition of glucose, including biomaterial could be acted as an insulator, thus, 40 μg/mL of Cu-nanoflowers was chosen. The enzyme activity is highly susceptive by the surrounding atmosphere, the current value at different pH condition was monitored (Fig. 4c). Since GOx shows the best performance at weak acid condition (~pH 5.0), and the hydrogen peroxide generating electron with HRP is more stable in low pH due to the occurrence of deprotonation under basic conditions [44], which confirms that the current was increased at low pH. Therefore, pH 5.0 was selected as an optimum pH for electrochemical sensing of glucose using Cu-nanoflower@AuNPs-GO NFs as an electrochemical sensor.

Under the optimized conditions, the prepared glucose sensor was also evaluated by electrochemical analysis to judge the analytical performance (Fig. 5a). Since the cathodic current is related to the amount of electron generated by the reaction between Cu-nanoflower@AuNPs-GO NFs and glucose, the electrochemical signal (peak II) intensities were gradually increased as the rising the amount of glucose. While the linear regression equation at low concentration range (0–0.01 mM) was $\mu A = 3656.4933x + 0.6867$ with a correlation coefficient of 0.9618 ($n = 3$), in the high concentration range (0.03–0.1 mM), linear regression equation was $\mu A = 636.3007x + 19.9981$ with a correlation coefficient of 0.9903 ($n = 3$). The detection limit was 0.018 μM calculated by the 3σ-rule (Fig. 5b). When it compares with other electrochemical glucose sensors, which were based on the NFs or nanomaterials, Cu-nanoflower@AuNPs-GO NFs represent better electroanalytical performance (Table S1).

Finally, the selectivity of developed Cu-nanoflower@AuNPs-GO NFs-based glucose sensor was validified through the chronoamperometry analysis under various ingredient which could disturb the interaction mutual target and sensor (Fig. 5c). It can be noticed that the current was not changed with the addition of another interferent such as ascorbic acid, saccharose, urea, NaCl, KCl and BSA. However, the current was remarkably increased only when glucose was injected, which illustrates that the Cu-nanoflower@AuNPs-GO NFs acted as a selective glucose sensor at a trace level of glucose. To evaluate the time-dependent stability of the prepared Cu-nanoflower@AuNPs-GO NFs electrode, 30 μM of glucose solution was analyzed for 20 days (Fig. 5d). When it compares with the first days, the current value still maintained 95% until 16 days, and even after 20 days it represents over 91%. This is because of the supported nanomaterials helping the long-term stability, and it means that the designed nano biosensor has potentials for the field use. Moreover, reproducibility test was conducted by chronoamperometry using single electrode for several times ($n = 3$). As shown in Fig. S12, the Cu-nanoflower@AuNPs-GO NFs showed excellent reusability after 6 cycle reuse. The reproducibility has no obvious decline when used for 3 times, and it maintained the activity about 82% after 6 times reuse. The reusability of Cu-nanoflower@AuNPs-GO NFs indicated that the Cu-nanoflower could retain the enzyme activity well and decrease the loss or inactivation of the enzyme after several times reuse. Recovery test was performed under conditions similar to real samples using FBS (Table S2). The concentration of glucose already known was added in the FBS, and their content was measured. At independent glucose concentrations (3, 15, 60 μM), CV measurement was performed and compared using the corresponding calibrated curve. The recoveries of glucose in the spiked samples were between 96.59 and 105.26%, respectively. This result means that the proposed methods could be utilized for determining the amount of glucose in a real sample.

4. Conclusions

In summary, Cu-nanoflower@AuNPs-GO NFs were fabricated on the

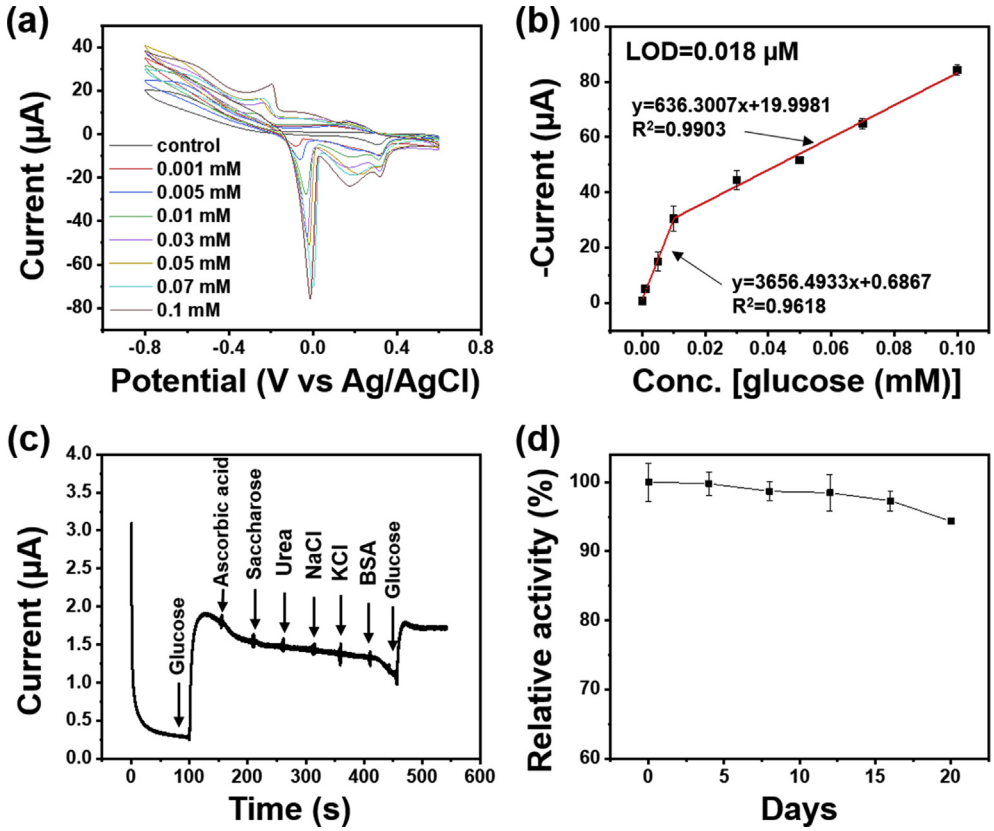

Fig. 5. (a) CV current measurement of different concentrations of glucose from 0 to 0.1 mM and (b) the corresponding calibration curve. (c) Dependence of current responses of Cu-nanoflower@AuNPs GO NFs for 50 μM glucose and other interferences. (d) Relative activity value during 20 days for stability test.

surface of Au chip and used as a promising electrochemical biosensor for the detection of glucose. The electrochemical properties of Cu-nanoflower@AuNPs-GO NFs were greatly improved due to the modification of NFs with GO, AuNPs and Cu-nanoflowers, yielding efficient electro-catalyzed reaction that converts glucose to gluconic acid at pH 5.0, which facilitates to increase current with increasing concentration of glucose. The Cu-nanoflower@AuNPs-GO NFs coated Au chip exhibited wider linear range (0.001–0.1 mM) with the detection limit of 0.018 μM for glucose detection. Furthermore, Cu-nanoflower@AuNPs-GO NFs coated Au chip electrode exhibited the best sensing performance than the NF based sensors for glucose detection. Thus, Cu-nanoflower@AuNPs-GO NFs coated Au chip could be used as promising electroanalytical tool for monitoring of glucose levels in biofluids for real-world clinical point-of-care testing.

Declaration of computing interest

To the best of our knowledge, the named authors have no conflict of interest, financial or otherwise.

Acknowledgments

Authors gratefully acknowledge financial support from the Ministry of Trade, Industry and Energy (Korea) under the Technology Innovation Program (20000773, Development of nanomultisensors based on wearable patch for nonhaematological monitoring of metabolic syndrome).

Appendix A. Supplementary data

Supplementary data to this article can be found online at https://doi.org/10.1016/j.msec.2019.110273.

References

[1] S. Yang, G. Li, D. Wang, Z. Qiao, L. Qu, Synthesis of nanoneedle-like copper oxide on N-doped reduced graphene oxide: a three-dimensional hybrid for nonenzymatic glucose sensor, Sens. Actuators B Chem. 238 (2017) 588–595.
[2] J. Wang, Electrochemical glucose biosensors, Chem. Rev. 108 (2008) 814–825.
[3] L. Chen, W.H. Tse, Y. Chen, M.W. McDonald, J. Melling, J. Zhang, Nanostructured biosensor for detecting glucose in tear by applying fluorescence resonance energy transfer quenching mechanism, Biosens. Bioelectron. 91 (2017) 393–399.
[4] J. Li, D. Kuang, Y. Feng, F. Zhang, M. Liu, Glucose biosensor based on glucose oxidase immobilized on a nanofilm composed of mesoporous hydroxyapatite, titanium dioxide, and modified with multi-walled carbon nanotubes, Microchim. Acta 176 (2012) 73–80.
[5] Z. Xing, J. Tian, A.M. Asiri, A.H. Qusti, A.O. Al Youbi, X. Sun, Two-dimensional hybrid mesoporous Fe_2O_3–graphene nanostructures: a highly active and reusable peroxidase mimetic toward rapid, highly sensitive optical detection of glucose, Biosens. Bioelectron. 52 (2014) 452–457.
[6] Y. Lv, Z. Zhang, F. Chen, Chemiluminescence microfluidic system sensor on a chip for determination of glucose in human serum with immobilized reagents, Talanta 59 (2003) 571–576.
[7] H. Yuan, W. Ji, S. Chu, S. Qian, F. Wang, J.F. Masson, X. Han, W. Peng, Fiber-optic surface plasmon resonance glucose sensor enhanced with phenylboronic acid modified Au nanoparticles, Biosens. Bioelectron. 117 (2018) 637–643.
[8] Y. Pei, M. Hu, F. Tu, X. Tang, W. Huang, S. Chen, Z. Li, Y. Xia, Ultra-rapid fabrication of highly surface-roughened nanoporous gold film from AuSn alloy with improved performance for nonenzymatic glucose sensing, Biosens. Bioelectron. 117 (2018) 758–765.
[9] L.M. Lu, L. Zhang, F.L. Qu, H.X. Lu, X.B. Zhang, Z.S. Wu, S.Y. Huan, Q.A. Wang, G.L. Shen, R.Q. Yu, A nano-Ni based ultrasensitive nonenzymatic electrochemical sensor for glucose: enhancing sensitivity through a nanowire array strategy, Biosens. Bioelectron. 25 (2009) 218–223.
[10] J. Yang, J.H. Yu, J. Rudi Strickler, W.J. Chang, S. Gunasekaran, Nickel nanoparticle–chitosan-reduced graphene oxide-modified screen-printed electrodes for enzyme-free glucose sensing in portable microfluidic devices, Biosens. Bioelectron. 47 (2013) 530–538.
[11] H. Zhao, X. Guo, Y. Wang, X. Duan, H. Qu, H. Zhang, D. Zhang, W. Pang, Microchip based electrochemical-piezoelectric integrated multi-mode sensing system for continuous glucose monitoring, Sens. Actuators B Chem. 223 (2016) 83–88.
[12] C. Chen, Q. Xie, D. Yang, H. Xiao, Y. Fu, Y. Tan, S. Yao, Recent advances in electrochemical glucose biosensors: a review, RSC Adv. 3 (2013) 4473–4491.
[13] S. Samavat, J. Lloyd, L. O'Dea, W. Zhang, E. Preedy, S. Luzio, K.S. Teng, Uniform sensing layer of immiscible enzyme-mediator compounds developed *via* a spray

aerosol mixing technique towards low cost minimally invasive microneedle continuous glucose monitoring devices, Biosens. Bioelectron. 118 (2018) 224–230.
[14] R. Wilson, A. Turner, Glucose oxidase: an ideal enzyme, Biosens. Bioelectron. 7 (1992) 165–185.
[15] S.J. Bao, C.M. Li, J.F. Zang, X.Q. Cui, Y. Qiao, J. Guo, New nanostructured TiO_2 for direct electrochemistry and glucose sensor applications, Adv. Funct. Mater. 18 (2008) 591–599.
[16] Y. Li, Y. Zhong, Y. Zhang, W. Weng, S. Li, Carbon quantum dots/octahedral Cu_2O nanocomposites for non-enzymatic glucose and hydrogen peroxide amperometric sensor, Sens. Actuators B Chem. 206 (2015) 735–743.
[17] M. Ma, T. Zhe, Y. Ma, Z. Wang, Q. Chen, J. Wang, Highly sensitive and reproducible non-enzymatic glucose sensor fabricated by drop-casting novel nanocomposite with 3D architecture and tailorable properties prepared in controllable way, Talanta 180 (2018) 133–143.
[18] B. Fang, C. Zhang, G. Wang, M. Wang, Y. Ji, A glucose oxidase immobilization platform for glucose biosensor using ZnO hollow nanospheres, Sens. Actuators B Chem. 155 (2011) 304–310.
[19] C. Hou, Y. Wang, Q. Ding, L. Jiang, M. Li, W. Zhu, D. Pan, H. Zhu, M. Liu, Facile synthesis of enzyme-embedded magnetic metal–organic frameworks as a reusable mimic multi-enzyme system: mimetic peroxidase properties and colorimetric sensor, Nanoscale 7 (2015) 18770–18779.
[20] M. Barbadillo, E. Casero, M.D. Petit-Domínguez, L. Vázquez, F. Pariente, E. Lorenzo, Gold nanoparticles-induced enhancement of the analytical response of an electrochemical biosensor based on an organic–inorganic hybrid composite material, Talanta 80 (2009) 797–802.
[21] P. Kannan, T. Maiyalagan, E. Marsili, S. Ghosh, L. Guo, Y. Huang, J.A. Rather, D. Thiruppathi, J. Niedziolka-Jönsson, M. Jönsson-Niedziolka, Highly active 3-dimensional cobalt oxide nanostructures on the flexible carbon substrates for enzymeless glucose sensing, Analyst 142 (2017) 4299–4307.
[22] Z. Lin, Y. Xiao, Y. Yin, W. Hu, W. Liu, H. Yang, Facile synthesis of enzyme-inorganic hybrid nanoflowers and its application as a colorimetric platform for visual detection of hydrogen peroxide and phenol, ACS Appl. Mater. Interfaces 6 (2014) 10775–10782.
[23] S.W. Lee, S.A. Cheon, M.I. Kim, T.J. Park, Organic–inorganic hybrid nanoflowers: types, characteristics, and future prospects, J. Nanobiotechnol. 13 (2015) 54–64.
[24] J. Sun, J. Ge, W. Liu, M. Lan, H. Zhang, P. Wang, Y. Wang, Z. Niu, Multi-enzyme co-embedded organic–inorganic hybrid nanoflowers: synthesis and application as a colorimetric sensor, Nanoscale 6 (2014) 255–262.
[25] X. Zhu, J. Huang, J. Liu, H. Zhang, J. Jiang, R. Yu, A dual enzyme–inorganic hybrid nanoflower incorporated microfluidic paper-based analytic device (μPAD) biosensor for sensitive visualized detection of glucose, Nanoscale 9 (2017) 5658–5663.
[26] J. Huang, Y. Liu, T. You, Carbon nanofiber based electrochemical biosensors: a review, Anal. Methods 2 (2010) 202–211.
[27] Z.M. Huang, Y.Z. Zhang, M. Kotaki, S. Ramakrishna, A review on polymer nanofibers by electrospinning and their applications in nanocomposites, Compos. Sci. Technol. 63 (2003) 2223–2253.
[28] N.L.T. Nguyen, S.H. Baek, Z.A. Akbar, S.-Y. Jang, S. Ha, J.P. Park, T.J. Park, Rapid determination of ethyl alcohol in alcoholic beverages using a fluorescent nanofiber film, BioChip J. 12 (2018) 240–248.
[29] S. Tripathy, S.R. Krishna Vanjari, V. Singh, S. Swaminathan, S.G. Singh, Electrospun manganese (III) oxide nanofiber based electrochemical DNA-nanobiosensor for zeptomolar detection of dengue consensus primer, Biosens. Bioelectron. 90 (2017) 378–387.
[30] M.H. You, X. Yan, J. Zhang, X.X. Wang, X.X. He, M. Yu, X. Ning, Y.Z. Long, Colorimetric humidity sensors based on electrospun polyamide/$CoCl_2$ nanofibrous membranes, Nanoscale Res. Lett. 12 (2017) 360.
[31] G. Yang, J. Wang, Y. Wang, L. Li, X. Guo, S. Zhou, An implantable active-targeting micelle-in-nanofiber device for efficient and safe cancer therapy, ACS Nano 9 (2015) 1161–1174.
[32] M.G. Katz, T. Wydeven Jr., Selective permeability of PVA membranes. I. Radiation-crosslinked membranes, J. Appl. Polym. Sci. 26 (1981) 2935–2946.
[33] Y. Xianda, W. Anlai, C. Suqin, Water-vapor permeability of polyvinyl alcohol films, Desalination 62 (1987) 293–297.
[34] A.G. Destaye, C.K. Lin, C.K. Lee, Glutaraldehyde vapor cross-linked nanofibrous PVA mat with *in situ* formed silver nanoparticles, ACS Appl. Mater. Interfaces 5 (2013) 4745–4752.
[35] L. Cao, F. Zhang, Q. Wang, X. Wu, Fabrication of chitosan/graphene oxide polymer nanofiber and its biocompatibility for cartilage tissue engineering, Mater. Sci. Eng. C 79 (2017) 697–701.
[36] M. Li, S.K. Cushing, X. Zhou, S. Guo, N. Wu, Fingerprinting photoluminescence of functional groups in graphene oxide, J. Mater. Chem. 22 (2012) 23374–23379.
[37] S. Thakur, N. Karak, Green reduction of graphene oxide by aqueous phytoextracts, Carbon 50 (2012) 5331–5339.
[38] G.K. Ramesha, S. Sampath, Electrochemical reduction of oriented graphene oxide films: an *in situ* Raman spectroelectrochemical study, J. Phys. Chem. C 113 (2009) 7985–7989.
[39] J. Xue, J. Xie, W. Liu, Y. Xia, Electrospun nanofibers: new concepts, materials, and applications, Acc. Chem. Res. 50 (2017) 1976–1987.
[40] Y.L. Wang, H. Yang, Z.L. Xu, Influence of post-treatments on the properties of porous poly (vinyl alcohol) membranes, J. Appl. Polym. Sci. 107 (2008) 1423–1429.
[41] H. Zhu, M. Zhang, S. Cai, Y. Cai, P. Wang, S. Bao, M. Zou, M. Du, *In situ* growth of Rh nanoparticles with controlled sizes and dispersions on the cross-linked PVA–PEI nanofibers and their electrocatalytic properties towards H_2O_2, RSC Adv. 4 (2014) 794–804.
[42] J. Ge, J. Lei, R.N. Zare, Protein–inorganic hybrid nanoflowers, Nat. Nanotechnol. 7 (2012) 428.
[43] L.D. Burke, T.G. Ryan, The role of incipient hydrous oxides in the oxidation of glucose and some of its derivatives in aqueous media, Electrochim. Acta 37 (1992) 1363–1370.
[44] C.Y. Park, J.M. Seo, H. Jo, J. Park, K.M. Ok, T.J. Park, Hexagonal tungsten oxide nanoflowers as enzymatic mimetics and electrocatalysts, Sci. Rep. 7 (2017) 40928.